

DYNAMIC SEISMIC RESPONSE OF LA MISSION BRIDGE IN BAJA CALIFORNIA, MÉXICO ¹

Song Hoon², Carlos I. Huerta-López³, Alejandro García-Gastélum⁴

ABSTRACT: The analytical and experimental seismic response of La Mission Bridge, and the site sub-surface characterization on its neighborhood is presented in this paper. SAP 2000 (Structural Analysis Program) was used to model and characterize numerically the expected response of the bridge in terms of their vibration natural frequencies and maximum displacement. It was also generated the scenario of the bridge response upon strong motion. In both cases, ambient vibration measurements were used for the experimental studies. The stiffness matrix method was used for the analytical study (forward modeling) of wave propagation in layered media. The relevant characteristics of the results are next succinctly described: For the bridge: the theoretical fundamental frequency of vibration was 3.10 Hz., and the estimated experimental fundamental vibration frequency was 3.30 Hz. For the site characterization, our results are described starting at the north end of the bridge going through its south end: (i) The site S1_2, which is the site where the soil was artificially compacted, has a dominant frequency of 2.5 Hz and an average shear wave velocity of 195 m/s. (ii) For sites S3_1 and S2_4, the dominant frequency was 1.5 Hz and the average shear wave velocity was 115 m/s and 123 m/s, respectively. (iii) Site S2_2, the dominant frequency was 3.5 Hz and an average shear wave velocity 275 m/s. (iv) Site S2_5, in this site two clear peaks at frequencies of 1.5 and 3.75 Hz were observed, regarding to the average shear wave velocity it was 128 m/s. (v) Site S2_3, the dominant frequency was 4.0 Hz and the average shear wave velocity was 346 m/s. All the experimental sites were in soils at natural conditions, but the site S1_2, which was artificially compacted. The soil characteristics along the 163 m length of the bridge, clearly shows a rigidity change of the soil sub-surface conditions. That condition is an indication that different amplifications of the ground response will probably be experienced, being in the range of the 4.0 Hz at the south-end side of the bridge, and 1.5 Hz on the portion of the north-end of the bridge. In no case the fundamental vibration frequency of the bridge matches the fundamental vibration frequency of the ground surface. However, they are somehow no too far apart each other.

Keywords: ambient vibration, natural frequency, layered media, shear wave velocity, dominant frequency

RESPUESTA SÍSMICA DEL PUENTE LA MISIÓN EN BAJA CALIFORNIA, MÉXICO

RESUMEN: La respuesta sísmica analítica y experimental del puente La Misión, en Baja California, México y la caracterización del terreno en la vecindad del puente se presenta en este artículo. Se utilizó el programa SAP 2000 para modelar numéricamente y caracterizar la respuesta esperada del puente en función de sus frecuencias naturales de vibración, sus desplazamientos máximos ante movimientos débiles y fuertes, así como las frecuencias de vibraciones teóricas y experimentales. Respecto del terreno, se utilizaron mediciones de vibración ambiental para su caracterización experimental. El análisis de la respuesta teórica del terreno se realizó mediante el modelado directo de la propagación del campo total de ondas que utiliza las matrices de rigidez para medios estratificados. De los resultados obtenidos sobresalen las siguientes

¹ Article received on March 29, 2022, and accepted for publication on April 15, 2022.

² Doctoral Student, Oceanological Research Institute (IO), Autonomous University of Baja California (UABC), Campus Ensenada B.C. México. Email: hsong@uabc.edu.mx

³ Associate Professor/Researcher, Civil Engineering and Surveying Department, University of Puerto Rico-Mayaguez (UPRM), Email: carlos.huerta@upr.edu, and Adjunt Professor, Faculty of Engineering Sciences and Technology, Autonomous University of Baja California (FCITEC-UABC), Campus Tijuana B.C. México. Email: m-huerta@alumni.utexas.net

⁴ Professor/Researcher, Faculty of Marine Sciences, Autonomous University of Baja California (UABC), Campus Ensenada B.C., México. Email: agarcia@uabc.edu.mx

características del puente (i) la frecuencia de vibración del modo fundamental del modelo del puente es de 3.1 Hz. El valor experimental estimado fue de 3.3 Hz. De la caracterización del terreno se da a continuación la descripción de los hallazgos: partiendo del extremo norte del puente (su inicio) hacia el extremo sur (final) del puente. Se observó que en el sitio S1_2 (parte norte) que es una zona compactada artificialmente, la frecuencia dominante es de 2.5 Hz, con una velocidad promedio de ondas de corte no mayor a 190 m/s. En los sitios intermedios S3_1 y S2_4 la frecuencia dominante estimada fue de 1.5 Hz y la velocidad promedio de ondas de corte varió respectivamente de 115 m/s a 123 m/s. En el sitio S2_2 se obtuvo una frecuencia dominante de 3.5 Hz y una velocidad promedio de ondas de corte 275 m/s. Para el sitio S2_5 se observaron dos picos espectrales, uno a 1.5 Hz y el otro a 3.75 Hz. Por otra parte, la velocidad promedio de las ondas de corte fue de 128 m/s. Finalmente, en el extremo sur del puente, para el sitio S2_3 se tiene una frecuencia dominante a 4.0 Hz y una velocidad promedio de las ondas de corte de 346 m/s. Todos los sitios donde se hicieron las mediciones experimentales están en condiciones naturales del terreno, a excepción del sitio S1_2 que fue compactado artificialmente. Lo antes descrito, muestra que a lo largo de los 163 m que tiene el puente, hay un claro cambio en la rigidez de los materiales del subsuelo y que el comportamiento esperado de la respuesta del terreno tenderá a amplificar significativamente los movimientos del terreno en el rango de frecuencias del orden de los 4 Hz en la porción sur del puente, mientras que para la porción norte del puente la amplificación significativa se espera pueda ocurrir alrededor de los 1.5 Hz. En ninguno de estos dos casos la frecuencia dominante de vibración del puente coincide con la del terreno circundante. Sin embargo, éstas no son muy diferentes unas de otras.

Palabras Clave: vibración ambiental, frecuencia natural, medios estratificados, velocidad de ondas de corte, frecuencia dominante

INTRODUCTION

The accelerated urban growth of border cities between California, USA and Baja California, México, as well as along the shoreline between San Diego-Tijuana-Ensenada (the largest bi-national conurbation shared between USA and México), and the construction on the Mexican side (government and/or private) of dwellings (whether authorized or not) high-rise condominium buildings, and industrial estates on hilltops and slopes has been ongoing for the last 40 years, but communication roads/highways between Tijuana and Ensenada. For example, for Tijuana the mean territorial expansion currently is 2.25 hectares/day, and the population grew at 4.7% on average annually. Overpopulation and rapid, unplanned urban development of the region both mean that human activity has become a key triggering factor in terrain instability. The economic activity of the border region, which includes San Diego-Tijuana-Rosarito-Ensenada depends mainly on the Tijuana-Ensenada scenic road, which was built in the early 60's.

The natural conditions due to the seismo-tectonic and geological conditions at which the region is exposed, as well as the known on-shore and off-shore mapped fault systems (related to the interaction between the North-America and the Pacific plates) are clear indications of the regional hazard at which all civil infrastructure is exposed.

Results of experimental and theoretical dynamic properties and response upon seismic loads, of La Mission Bridge (located at Km 50+1 on the scenic road Tijuana-Ensenada), as well as soil-site characterization in its neighborhood are here presented. Ambient Vibration (AV) measurements of the structure and the free-field were collected and digital signal processing (DSP) spectral analysis were conducted for the estimation of the experimental vibration frequencies of the bridge, and the horizontal to vertical spectral ratio (HVSr) for the site vibration frequencies characterization. For the estimation of theoretical vibration frequencies and response of the bridge to weak and strong ground motions, the code SAP2000 (which solves the Eigen-value problem considering the geometry, and the physical properties of the structural elements) was used. For the soil-site characterization, forward modeling by means of the stiffness matrix method developed by Kausel and Roesset (1981), was used.

LA MISSION REGION AND LA MISSION BRIDGE DESCRIPTION

La Mission Bridge

The characteristics and dimensions of the studied bridge are: (i) 163.26m of length and 23.50m wide of deck including the guardrail, (ii) bridge beams are type V of AASHTO, (iii) piers as supporting at intermediate points, (iv) the left shoulder is an abutment (Tijuana-Ensenada direction), and (v) the right shoulder is an abutment with deep pile foundation (Ensenada-Tijuana direction). Figures 1 and 2 provides auto-cad figures of profiles and cross sections, and pictures of the bridge and its structural elements, respectively. The bridge physical descriptions are next provided.

The spans between abutments and piers of the five sections of La Mission bridge are:

- Left shoulder - Pier 1 (beam one): 32.65m;
- Pier one – Pier 2 (beam two): 32.65m;
- Pier two – Pier 3 (beam three): 32.65m;
- Pier three – Pier 4 (beam four): 32.65m;
- Pier four – Right shoulder (beam five): 32.55m

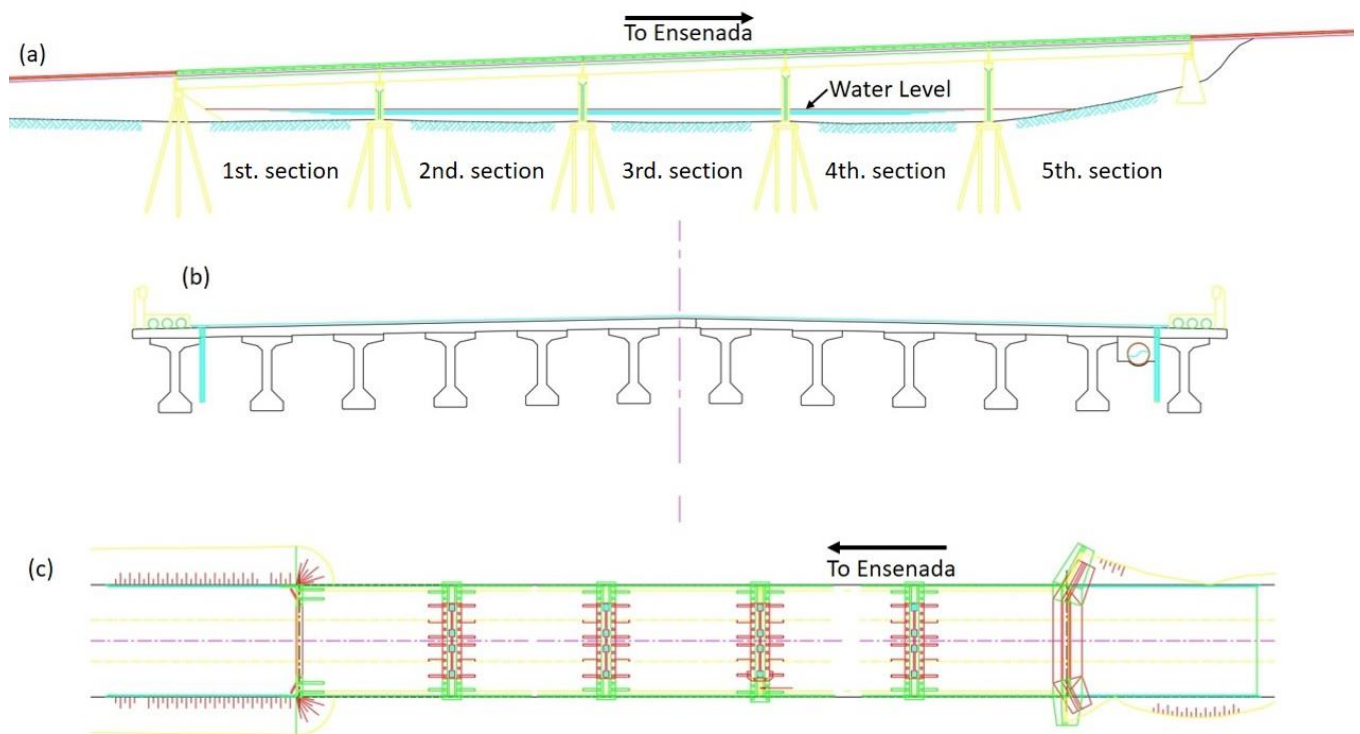


Figure 1: La Mission Bridge.

(a) longitudinal profile bridge, (b) Transverse Cross-Section of superstructure bridge, and (c) Plane of bridge.

The bridge has a slope approximately of four percentage (4%) in Tijuana-Ensenada direction. The deck is a continuous 20 cm thickness reinforced concrete all along the bridge. The beams are perforated pre-cast and pre-stressed independent structural elements, separated at each supporting pier. Neoprene plates were placed at each supporting pier location, acting as an articulation. Because the beams are discontinuous no moments are produced, but axial loads.

Along the wide direction of the bridge deck (23.50m) at 1.97m, 12 beams type V of AASHTO were placed in each section, because there are 5 sections a total of 60 beams type V of AASHTO were installed. At each one third of each section, diaphragms were constructed to provide lateral rigidity.

Deep pile foundation was installed in each intermediate pier and at the right shoulder. In the right shoulder, an array of 12 piles was installed as follows: three at each end, one vertical and two non-vertical at 15°, and groups of three vertical deep pile foundation at each 1.97m. In each intermediate pier (piers: one, two, three, and four), 4 piles were installed as follows: four at each end (two vertical and two non-vertical at 15°), and groups of two vertical piles at each 1.97m. Each pier has 38 deep pile foundation, giving a total of 126 deep pile foundation for the whole bridge.



Figure 2: La Mission Bridge. (a), (b) and (c) Road view, (d) pier view and (e) neoprene plates.

La Mission Region Description

The site is located in the area named as La Mission, showing either historical or recent earthquake activity, which is a consequence of the regional relative motion between the North-American and the Pacific Plates. The region is characterized for several well identified and mapped regional and local fault systems shown in Figure 3, which also shows the catalog of epicentral locations of historical $M > 6$ earthquakes, as well as all $M > 2$ instrumental detected seismicity up to 08/2017. Either the historical and instrumental documented seismic activity, was compiled from the seismological agencies: (i) *Red del Noroeste de México (RESNOM)* from the 1970's, and the (ii) Southern California Seismic Network (SCSN) from the 1960's.

The potential occurrence of $M > 6$ earthquakes in the region, is clearly shown in Figure 3, and from the compiled information of earthquakes catalog geographically filtered for the Northern Baja California – Mexico, and Southern California –USA regions and the temporal window of 1970's to 08/2017, and 1932 to 08/2017, respectively.

The relationship between the epicentral locations and the mapped faults (or fault zones) clearly shows the ones that are more seismic active in the whole region. The regional structural-tectonic frame in the neighborhood of the studied region, shown in Figure 4, is formed by: (i) at the North by the: Rose Canyon, la Nacion, Agua Caliente, Garcia, Vallecitos-San Miguel, Los Buenos, Miramar, and Coronado Bank (off-shore), and (ii) at the South by the: Agua Blanca, Tres Hermanos, San Diego Through and San Clemente, both West-South-West off-shore. The historical and local seismic activity in the vicinity of La Mission region is low in comparison with the rest of the region.

GEOLOGICAL DESCRIPTION OF LA MISSION REGION

The site in which the studied structure (bridge) is located, is within a region characterized by parallel normal faults (horst-graben systems) along the shore-line forming plateaus. In the work of Minch *et-al* (1984), a detailed description of the Miocene for the Northwestern Baja California Peninsula is provided about the stratigraphy and depositional ambient of the California-Baja California Continental Borderland.

The Rosarito Beach formation unit and is correlated lithological units were deposited within the California-Baja California Continental Borderland and the Range provinces. The Rosarito Beach shows a great variety of lithology and fauna that goes from sub-aerial basalt flows, pyroclastic sediments (Loophole, Tuff, Volcanic ash, Lapilli tufs), as well as diatomaceous sediments, sandstone tuff, conglomerates, and coquina with abundant invertebrate mega-fossils as gasteropods, pelycypods, crustaceans, and vertebrates as fish, birds and mammals. There is also, abundant diatomaceous siliceous micro-fossils, silico flagellates and radiolarian by Demere *et-al*. (1984). The Rosarito beach formation, is divided in seven units, based in its lithology and fauna variations by Minch *et-al*. (1984), being La Mission and Los Indios the subsoil lithological units present at the studied site, in which Quaternary Alluvial sediments formed by gravel, sands, clay and silt rests. The basalts and pyroclastic rocks of Rosarito Beach formation are exposed all along the shore-line between Tijuana and Ensenada, forming plateaus within the La Mission region, and covering a local area, which is representative of the period of explosive volcanic episodes during the Mid-Miocene and the early stage of the formation of the California-Baja California Continental Border line during the Miocene.

Seismicity and Local Geology

The study area is clearly evident tectonic active in terms of its seismic activity. As an example, according to RESNOM, during 04/28/1982 to 12/13/2008, 118 earthquakes of $0.6 \leq M \leq 4.1$ occurred in La Mission area. Figures 3 and 4, show the local and regional mapped faults, as well as the epicentral locations nearby the studied site.

Locally, in the studied site at La Mission area, the surficial layers are of alluvial deposits produced by the erosion and weathering of the typical intrusive igneous rocks of the region. The geomorphological relief of the region shows a quite flat topographic relief. On Figure 5, the location of the studied bridge, the regional and the local geological conditions are shown.

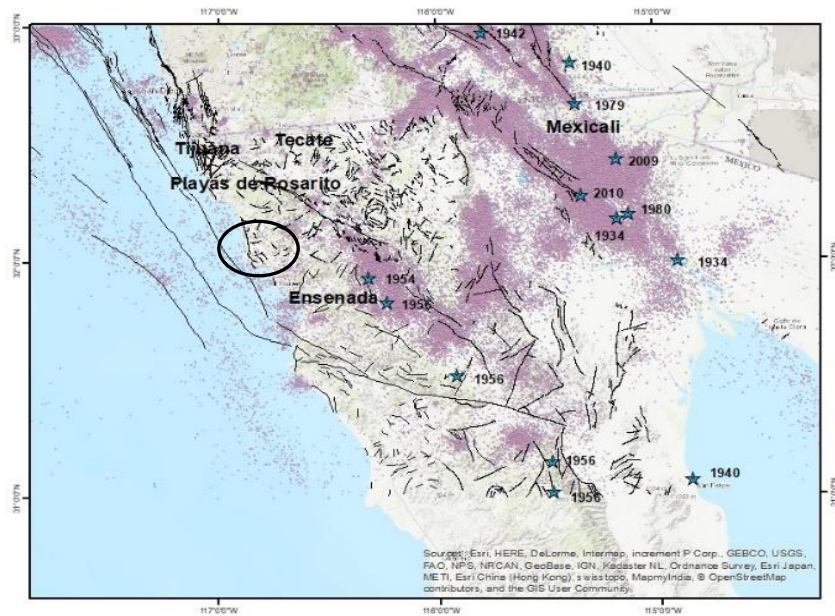


Figure 3: Principal northern Baja California, Mexico urban centers. Regional and local northern Baja California, Mexico and southern California, USA fault systems. Black oval show la Mission region. Stars show the historical $M \geq 6$. earthquakes, and small pink dots the accumulated all magnitudes seismicity from 1932-2017 (august). Source of epicentral locations: *Red Sísmica del Noroeste de México (RESNOM)*, Southern California Seismic Network (SCSN) and United States Geological Survey (USGS).

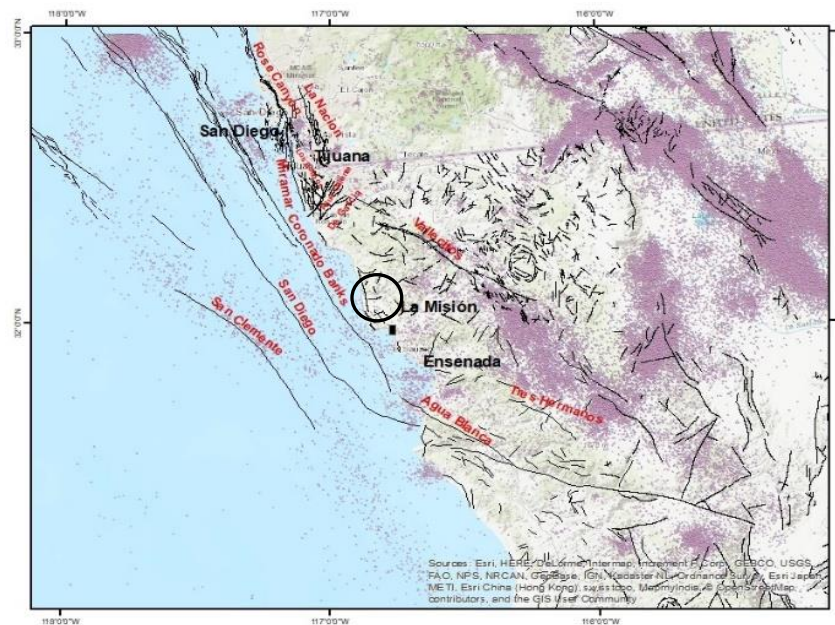
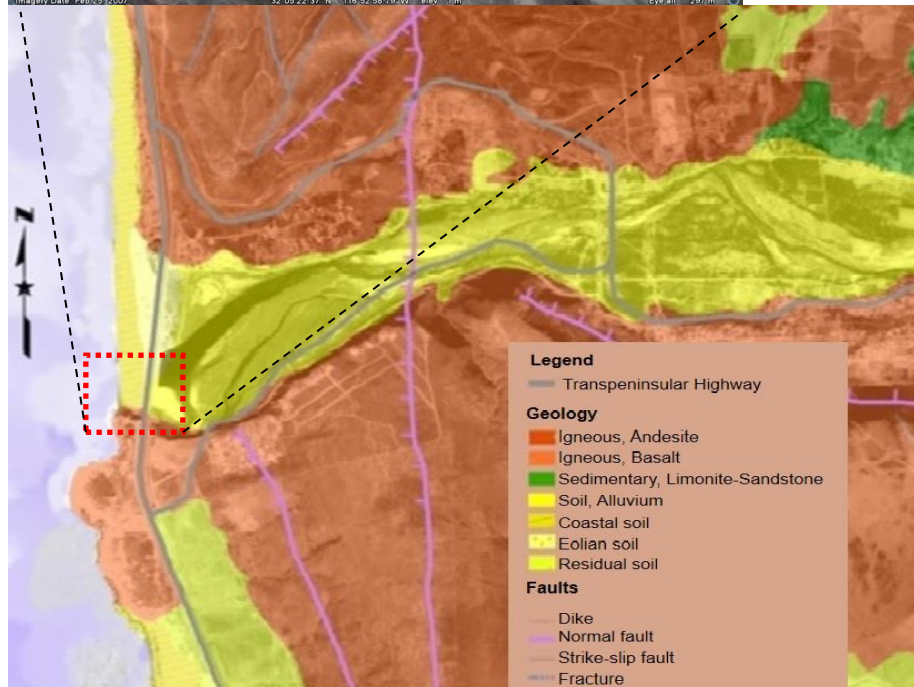


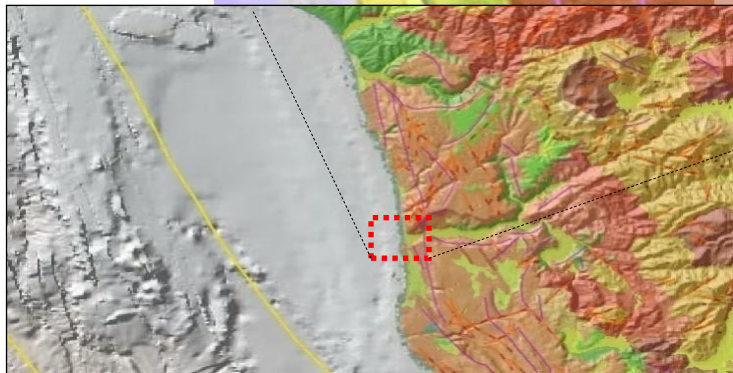
Figure 4: Regional structural frame work of La Mission Region, the accumulated seismicity reported by RESNOM and USGS for 1973 to 2017 (august) is shown in pink solid dots. The study site is shown with black oval, and faults with black lines.



(a)



(b)



(c)

Figure 5: Regional geology of studied site, La Mission Bridge. (a) Bridge location, (b) Local geology at La Mission Bridge, and (c) Regional geology.

DATA PROCESSING AND MODELING

Numerical Modeling for the Soil-Site Characterization

The wave propagation Stiffness Matrix method developed by Kausel and Roesset (1981) was used for the site-soil forward modeling of layered media. The Stiffness Matrix method is essentially a modified wave propagation method developed by Thomson (1950) and Haskell (1953). It is a more efficient code that works in a similar way as codes used in structural analysis. Here, the main purpose of using the Stiffness Matrix method is the sub-soil-site characterization in terms of the: (i) geometry and physical properties of layered soil system, (ii) dominant vibration frequency, and (iii) its transfer function in the frequency domain.

The analysis and characterization of layered soil system response was conducted by means of the 1-D wave propagation method based on the stiffness matrix. This linear wave propagation method, developed by Kausel and Roesset (1981), was used because among of its particular numerical and computational features, it provides the freedom of:

- (i) Use the total wave field (P, SV, SH) or any of particular interest of them,
- (ii) Can be used for modeling thin layers in the layered soil systems,
- (iii) Normal and non-normal incident wave field at the soil system-half space interface can be used,
- (iv) The behavior of the propagation wave field through and at the interfaces of the layered soil system can be traced.

As a final step, this method was implemented in a code written in Fortran language to estimate the site shear-wave velocity profile versus depth as developed by Kausel and Roesset (1981), and implemented by Huerta López et al., (2005).

Numerical Study of “La Mission” Bridge

In SAP 2000, before the analytical model is developed, it is necessary identify and compute the centroidal axis of structural elements, it is said: beams, piers, deck, abutments, and shoulders, among others.

Before the bridge structural elements are developed the following steps should be conducted: (i) the first step is to design the grid for easy location of structural elements, and then (ii) according to the design specifications the structural elements are developed. As an example, to develop a type V AASHTO beam, the SAP 2000 protocol is: Define > SectionProperties > Framesections > AddFrameProperty > Framesectionpropertytype > Concrete > Precast I > Set SectionDimensionshellon a Standard Section > AASHTO Beam I – Type V > Ok.

For the case of shear wall and/or the deck the *shell* function should be used. Once all the bridge structural elements are developed (following the design specifications of the structural maps), the nodes of the deck and beams should be joined as a rigid element with no weight or by using the function “*constraint*” of type “*body*”.

For this study case, rigid elements with no weight were used. As mentioned before, because the beams are discontinuous elements, the function “*AssignFrameReleases*” was used to release the moments. Once the whole bridge structure was developed, the code was executed to obtain the nodal results.

Collecting and Processing of Experimental Data

The collected data was recorded in raw binary format (.SSR) in counts digital units. In preparation for the digital signal processing (DSP) data was converted to acceleration (by applying the joint sensor-recorder constant of $3.8147 \times 10^{-6} \text{ g(m/s}^2\text{)/counts}$) physical units and converted to ASCII format.

The first step for the data processing consisted in time domain visual inspection of the time series plots, in order to identify non characteristic ambient vibration signals (anthropogenic undesired vibrations) for manually removal. Our DSP procedure does not require the transient signals being manually removed.

The frequency domain analysis was conducted by computing the Power Spectral Density (PSD), mean removal and base line correction was first applied to the time series. Instrument correction was not needed to apply due that the transfer function frequency response of the accelerometers is within \sim DC-200 Hz, wide enough of the frequency band of our interest.

PSD estimation was conducted following the standard Fourier analysis as described on signal processing books like: Kanasewish (1981), Oppenheim and Shafer (1975), and Bendat and Piersol (1971). PSD were estimated using time series of 86272 total length of data points using sub-segments of 4096 points with overlap of 50% and 75% until complete the total data length of the recorded time series. The more stable PSD's were the ones obtained with the largest overlap.

The mean value of each sub-segment was removed and Hanning window of equal number of points was applied to each sub-segment either. Final spectral amplitudes of the average PSD was normalized by the frequency increment (Δf) and the amplitude scaling factor (due to the symmetry of the discrete Fourier Transform) divided by the data points number (N). Appendix A provides details for the Discrete Fourier Transform (DFT) analytical derivation. Details of description provided above are in the Appendix A.

NAKAMURA H/V SPECTRAL RATIO ESTIMATION

The horizontal to vertical spectral ratio (HVSr) using ambient vibration (AV) as developed by Nakamura (1989), is an efficient and well proved method for the estimation of fundamental vibration mode of soil systems.

The Nakamura's fundamental hypothesis is based on empirical observations of computed HVSr that allows the estimation/identification of the fundamental vibration mode, which at the same time is interpreted an indicator of the local site response. He also states that by doing the HVSr the source and path effects are canceled (minimized) and the Rayleigh waves on the ambient noise. The hypothesis also implies that for small strains of the ground motions (site response) on vertical component are not significantly affected by the soft materials that constitute the soil.

The data acquisition field work for the Nakamura HVSr method requires ambient vibration (micro-tremors) measurements at single location with an orthogonal sensors array deployed at the ground surface. Its general hypothesis states that in rigid soils (rock) the ground response of horizontal and vertical components are very similar, which can be interpreted that there is no preferential direction of particle motion in the wave propagation phenomena, and that any observed amplification at the ground surface is a consequence of the presence of soft soils and can only be explained because the previous statement.

The academic community widely accepts the fundamental hypothesis of the Nakamura method, Nakamura (1989), which states that both the horizontal and the vertical ambient vibration signals are amplified independently from multiple reflections of shear- and compression-waves, respectively. Even though the debate about if the local site response is due to Surface Rayleigh waves still on discussion among the academic community, Nakamura (2000), and Huerta-Lopez *et al.* (2003) provides evidence that the contribution of surface Rayleigh waves has little or no contribution at the fundamental vibration mode.

EXPERIMENTAL HVSR COMPUTATIONS

To compute the hvrs from ambient vibration by nakamura (1989) psds computed as described in section of collecting and processing of experimental data, and carefully analyzed as described in sub-section nakamura h/v spectral ratio estimation. We used series of scripts written on the matlab environment following the procedure described by chatelain et al. (2008) and documented on sesame (2004) project. The quadratic arithmetic mean of both horizontals h1 and h2 psds, and the vertical v psd were use to estimate the final hvsr, as stated in equation (1):

$$R = \frac{\sqrt{\frac{H_1^2 + H_2^2}{2}}}{V} \quad (1)$$

RESULTS: ANALYSIS AND COMPARISON

Bridge Comparison of Numerical and Experimental Results

Figure 6 provides the location of sensors array deployed on the bridge sections, associated with the node of the finite element model, while Figure 7 shows both the theoretical pseudo-spectral acceleration of longitudinal, transversal, and vertical (PSA at 0%) and the experimental PSDs estimated from the two Ambient Vibration (AV) measurement campaigns.

The first column on Figure 7, corresponds to the longitudinal (first row), transversal (second row) and vertical (third row) of PSDs and PSAs of bridge first section. On same Figure 7, second, third, and fourth columns correspond to the second third and fifth bridge sections, following the same order described above.

Figure 7 shows the following: (i) First column-bridge first section, show good agreement between PSDs and PSAs at 3.25 Hz, the fundamental vibration frequency (FVF) for longitudinal, transversal and vertical components. On the transversal component, a second PSA peak at 4.3 Hz peak is not evident on the longitudinal and the vertical PSDs, (ii) Plot second column-bridge second section, show good agreement between PSDs and PSAs at the FVF for longitudinal, and transversal components at 3.2 Hz but for vertical component where the PSA is slighted shifted to 3.65 Hz, (iii) Plot third column-bridge third section in a very similar way of bridge second section, the results show good agreement between PSDs and PSAs at the FVF for longitudinal, and transversal components (3.2 Hz) but for vertical component where the PSA is slighted shifted to 3.65 Hz, (iv) Plot fourth column-fifth bridge section show good agreement between PSDs and PSAs at the FVF for longitudinal, transversal and vertical components (3.25 Hz).

Regarding to the FVF, the best agreements (almost perfect match) were obtained for all longitudinal components in all bridge sections. For the transversal components a second PSA peaks are shifted to high frequencies from the FVF, which is not present in the PSDs is evident in all bridge sections. On the vertical component good agreement was obtained for first and fifth bridge sections, but for second and third bridge sections in which the FVF of PSA is shifted to high frequencies from the FVF.

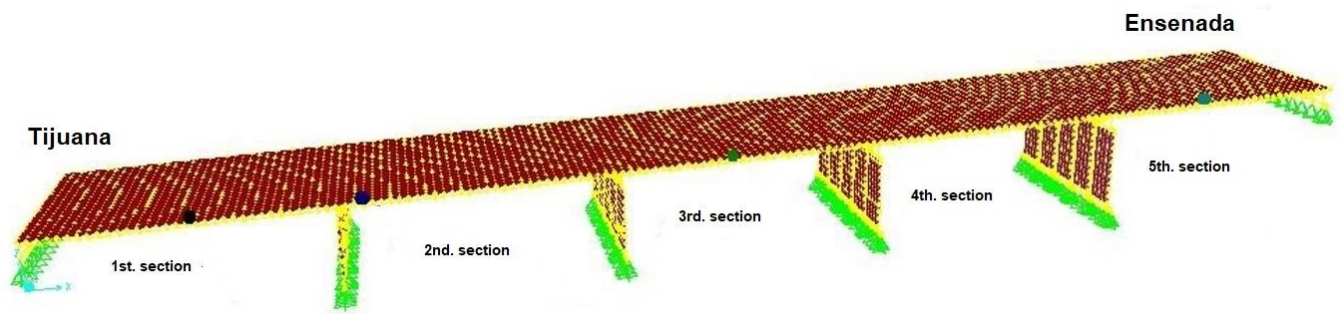


Figure 6: La Mission Bridge sensors array location with the associated node of the structural elements of the bridge sections.

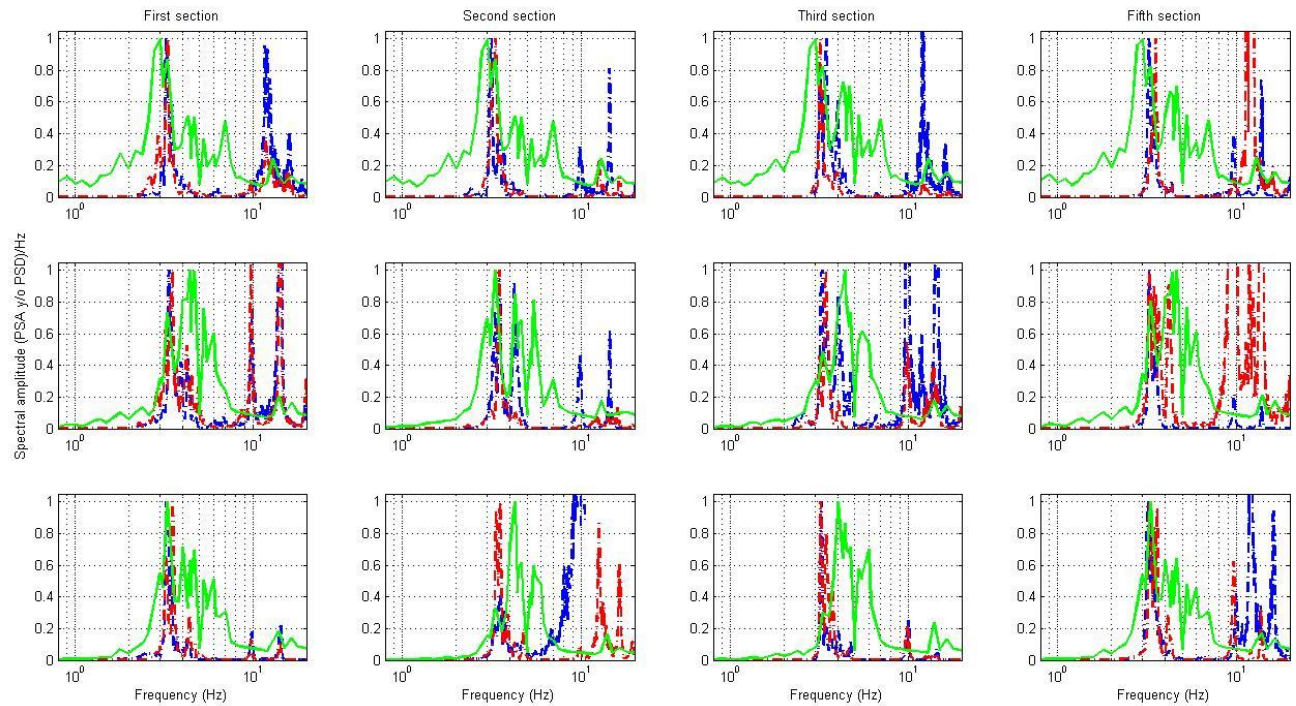


Figure 7: Experimental PSD spectrum and theoretical PSA, both are normalized with respect to its maximum. Longitudinal (first row), transversal (second row) and vertical (third row). Green line is the theoretical PSA. Dashed blue line data from first measurements campaign, and dashed red line the second measurements campaign.

Site Characterization: Comparison and Interpretation of Theoretical and Experimental HVSRS

This section describes the site characterization in terms of the pseudo-transfer function obtained by means of SRHV at the free-field locations shown in Figure 8, and the site physical properties and geometrical layered soil models from the numerical results of the 1D wave propagation modeling by means of the stiffness matrix method by Kausel and Roesset (1981) described in section of numerical modeling for the soil-site characterization.

Experimental results of PSDs H/V [Average of L/V and T/V] (H_{N-S}/V [L/V], H_{E-W}/V [T/V]), as well as the theoretical spectral ratios of H_{SH}/P [SH/P], and H_{SV}/P [SV/P] obtained by the stiffness matrix method by Kausel and Roesset (1981) are provided in Figure 8. The results for free-field modeled sites layered soil system of: (i) physical parameters, and (ii) geometry are provided in Table I.

Site S1_2 is shown in Figure 8, and the results are provided in Figure 9 “first column-first row”. Clear and good agreement of both experimental and theoretical spectral ratios is observed at 2.5 Hz. However, the modeled transfer function did not match the experimental ratios at frequencies larger than 4 Hz. Site S3_1 is shown in Figure 8, and the results are provided in Figure 9 “second column-first row”. The FVF is shown at 1.5 Hz with very good agreement between the SH/P and the T/V . Both experimental and theoretical spectral ratios preserves the general trend among them at frequencies range of 4 Hz up to 7 Hz. Site S2_4 is shown in Figure 8, and the results are provided in Figure 9 “second column-second row”. In both, experimental and theoretical spectral ratios, good agreement of two clear amplitude peaks are observed at 1.5 Hz and 3.8 Hz (4 Hz in the theoretical). Site S2_5 is shown in Figure 8, and the results are provided in Figure 9 “third column-first row”. On the experimental spectral ratios, two spectral amplitude peaks are observed at 1.5 Hz and in the range of 3 to 5.3 Hz. On the theoretical spectral ratios, the spectral amplitude are observed at 1.5 Hz and 3.9 Hz, Both results, theoretical and experimental agrees well for the 1.5 Hz, and quite well for the one on the range of 3 to 5.3 Hz with the theoretical at 3.9 Hz. Site S2_2 is shown in Figure 8, and the results are provided in Figure 9 “third column-second row”. A dominant spectral amplitude peak is observed at 4 Hz and a second spectral amplitude peak of lower amplitude at 9Hz. The general trend between both, the theoretical and the experimental spectral ration shows good agreement. Site S2_3 is shown in Figure 8, and the results are provided in Figure 9 “fourth column-first row”. For the theoretical spectral ratios, the largest spectral amplitude is located at 4 Hz, followed by a second one with lower amplitude at 9.5 Hz. For the experimental spectral ratios the largest spectral amplitude is located at 4 Hz, followed by a second one with lower amplitude at 7 Hz. The general trend between both, the theoretical and the experimental spectral ration shows good agreement.

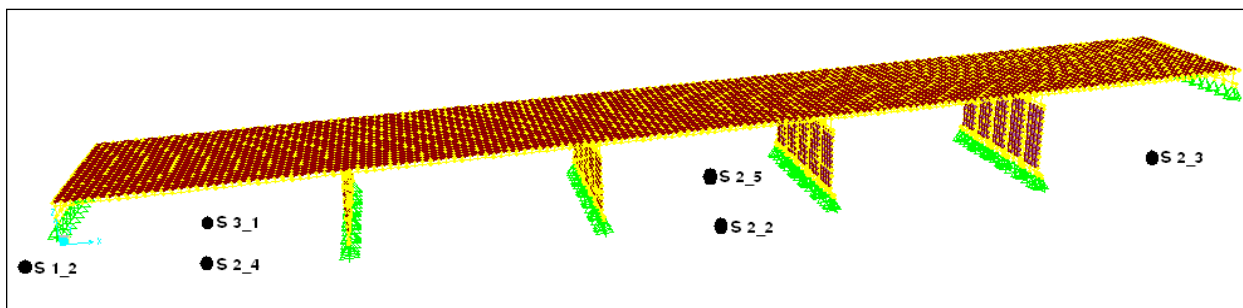


Figure 8: Free-field sensors array configuration nearby La Mission Bridge. S1_2 located at the beginning of the bridge on artificially compacted soil, S3_1 located at 11.9m on longitudinal direction and at 6.3m on transversal direction, S2_4 located on soil natural conditions at central point of first section, S2_5, and S2_2 located in soil natural conditions at longitudinal and transversal central point of third section, S2_3 located half way of fifth section on natural soil conditions.

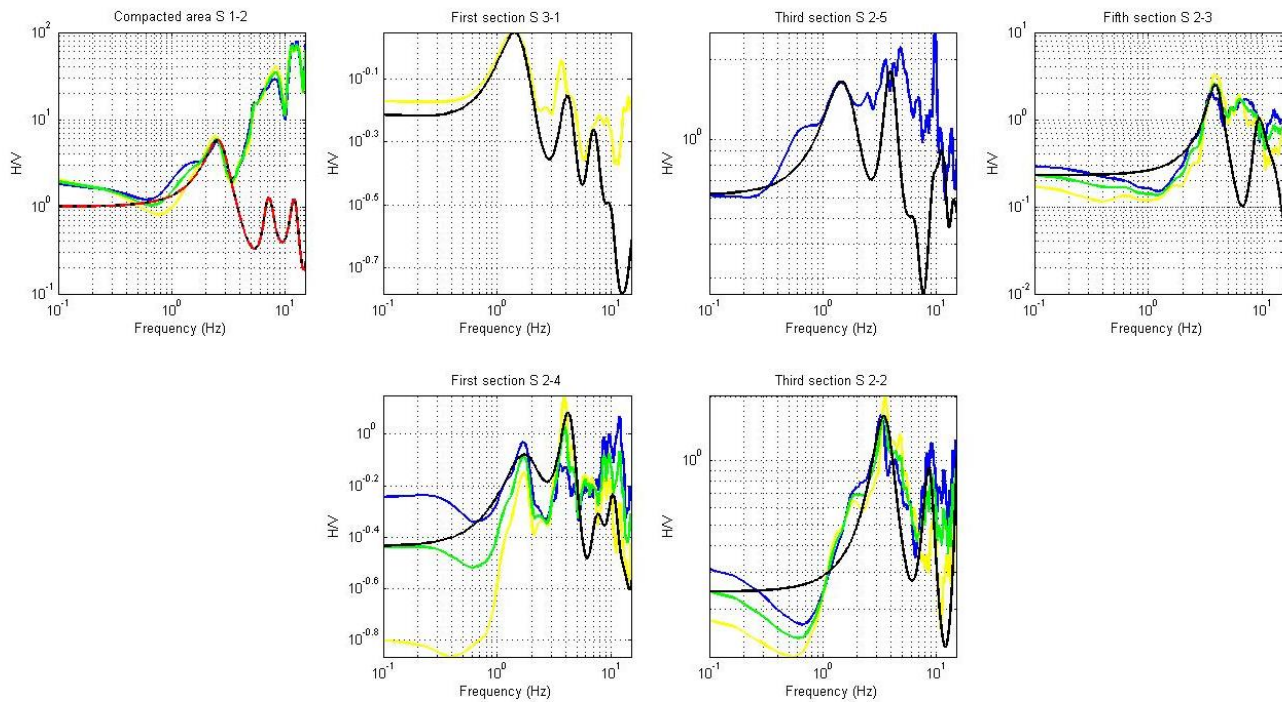


Figure 9: Free-field sites experimental spectral ratios, L/V, T/V, and H/V; and theoretical SV/P and SH/P spectral ratios. Blue line L/V spectral ratio. Yellow line T/V spectral ratio. Green line H/V spectral ratio. Black line SV/P spectral ratio, and dashed red line SH/P spectral ratio.

Table 1: Free-field sites modeling results: sites estimated physical properties, geometry, and average values for an equivalent single layer model.

Site	h (m)	V_s (m/s)	ρ (tn^*seg^2/m^4)	ξ (%)	σ	f_d (Hz)	\bar{V}_s, \bar{h}
S 1_2	7	170	0.1569	0.04	0.30		
	13	210	0.1627	0.02	0.40	2.5	196, 20
	0	550	0.1850	0.0	0.25		
S 3_1	7	100	0.1500	0.10	0.30		
	13	122	0.1600	0.10	0.40	1.5	114.3, 20
	0	200	0.2000	0.0	0.25		
S 2_4	7	100	0.1500	0.05	0.26		
	13	135	0.1700	0.09	0.36	1.5	122.75, 20
	0	200	0.1850	0.0	0.25		
S 2_5	7	100	0.1500	0.035	0.29	1.5	128.083, 24
	13	138	0.1600	0.045	0.38		

	4	145	0.1800	0.025	0.29		
	0	200	0.2000	0.0	0.25		
S 2_2	2.6	200	0.1500	0.05	0.26		
	7	220	0.1600	0.06	0.35		
	7.4	350	0.1700	0.03	0.37	3.5	274.859, 21.4
	4.4	280	0.1700	0.033	0.38		
	0	800	0.2000	0.0	0.25		
S 2_3	3	100	0.1500	0.05	0.26		
	7	175	0.1800	0.05	0.28		
	6.5	450	0.1850	0.005	0.28	4.0	346.511, 21.5
	5	600	0.1900	0.005	0.26		
	0	970	0.2000	0.0	0.25		

ρ : density, ξ : damping, σ : Poisson ratio, V_s : shear-wave velocity, h : thickness, f_i : fundamental vibration frequency, \bar{V}_s : average shear-wave velocity, \bar{h} : average thickness

CONCLUSIONS

Site characterization nearby La Mission Bridge most relevant issues are documented on Table I and next described as follows: (i) Free-field sites nearby to bridge first and second sections shows FVF lower than sites nearby bridge sections three and five, (ii) at site S1_2 the associated FVF is 2.5 Hz, while at sites S3_1 and S2_4 the FVF is 1.5 Hz, (iii) on the site S2_2 (facing to the sea) the FVF is 3.5 Hz, and 1.5 Hz for the site S2_5 (facing to the lagoon), these two sites are nearby the bridge third section, just at the middle of the bridge, (iv) for site S2_3 (nearby the bridge fifth section) the FVF is 4 Hz, which is the most rigid soil conditions of the soil along the bridge.

Regarding to results description provided in section Bridge comparison of numerical and experimental results, the bridge experimental (PSDs), and theoretical (PSAs) mean value of the FVF estimated on all bridge sections is 3.15 Hz, and 3.10 Hz, respectively. These values are close enough for its use in the analysis of the dynamic behavior of civil structures to estimate the experimental structural dynamic behavior using AV measurements.

DATA AND RESOURCES

We used time series of ambient vibration (AV) measurements collected with epi-sensor accelerometers from the engineering, architecture, and design faculty of UABC-Ensenada. Seismic catalogs can be obtained from <https://resnom-mf.cicese.mx/>, and Southern California Seismic Network (SCSN) and United States Geological Survey (USGS). MATLAB is available at www.mathworks.com/products/matlab (last accessed July, 2020). Geology (home-vectorised data) for the northern Baja California were obtained from INEGI web-site <https://www.inegi.org.mx>. SAP2000 V10., (2000) Computers and structures, Inc.

ACKNOWLEDGMENTS

This study was supported by the Mexican National Council of Science and Technology (CONACyT) and the doctoral scholarship of Hoon Song at the *Universidad Autónoma de Baja California*. We are grateful to the Puerto Rico Strong Motion Program of the Civil Engineering and Surveying Department of the University of Puerto Rico for supporting Hoon Song during his stay at the University of Puerto Rico as student exchange and the student's mobility program of CONACyT. This manuscript has benefited from thoughtful suggestions and detailed comments by our reviewers and the anonymous reviewers for valuable suggestions. To the *Secretaría de Transporte y Comunicación* (SCT) authorities for their invaluable support detouring the vehicles traffic while collecting the AV data.

REFERENCES

- Alfaro A., Goula X., Susagna T., Pujades L. G., Canas J. A. Navarro M. and Sánchez J. (1998). *Estimación del Período Predominante del Suelo a Partir de Microtemblores*, Aplicación a Barcelona, IX Asamblea Nacional de Geodesia y Geofísica, Aguadulce (Almería, España), Febrero 9-13.
- Alain W., Le Page M., Chávez V. G., Vela G. R., Castañeda S. R., and González V. C. (2000). *Aportes para un escenario sísmico en Tijuana, ¿y si un terremoto de magnitud 6.5 se produjera en la falla La Nación?*, El Colegio de la Frontera Norte y el Institut de Recherchepour le Développement, 74 p.
- Bendat, J. S., and Piersol A. G. (1971). *Random data: Analysis and measurements procedures*, John Wiley & Sons, Inc. New York, 407 p.
- Chatelain J. L., Guillier B. F. C., Duval A. M., Bard K. A. P. Y. and The WP02 SESAME team. (2008). *Evaluation of the influence of experimental conditions on H/V results from ambient noise recordings*, Bull Earthquake Eng. 6: 33–74 p.
- Chopra Anil K. (2007). *DYNAMICS OF STRUCTURES-Theory and Applications to Earthquake Engineering*, Third Edition, Prentice Hall. 1 – 48, 208 – 212, 244 – 245 p.
- Demere T.A., Roeder M. A., Chandler R.M., and Minch J. A. (1984). *Paleontology of the Middle Miocene Los Indios Member of the Rosarito Beach Formation, Northwestern Baja California, Mexico*; Minch J.A., Ashby J.R. (eds.), *Miocene and Cretaceous Depositional Environments, Northwestern Baja California, Mexico*, Pacific Section A.A.P.G., San Diego, California, 54, 47-56 p.
- Esparza Fuentes M., Huerta López C. I., Lomelí Limón D. S., Baltasar Cifuentes Y., Contreras Porras R. S., Espinoza Barreras F., and Song H. (2007). *Theoretical and experimental vibration frequencies of a nine story building located near the Tijuana's river zone* (Estimación teórica y experimental de la vibración de un edificio de nueve niveles localizado en la vecindad de la zona río de Tijuana, B.C.), Memorias del XVI Congreso Nacional de Ingeniería Sísmica, Ixtapa Zihuatanejo, México. Oct/31-Nov/3, 2007, CD proceedings paper Nov-14, 1-19 p.
- Espinoza Barreras F., Huerta López C. I., Juárez García J. R., Contreras Porras R. S., Reynaga Márquez A., Ramírez González E., González Ortega J. A., Baltasar Cifuentes Y., Figueroa Martínez M., and Baltasar Rodríguez R. (2007). *Ambient vibrationson Ensenada B.C. urban bridges* (Vibración ambiental en puentes urbanos de Ensenada, B.C.), Memorias del XVI Congreso Nacional de Ingeniería Sísmica, Ixtapa Zihuatanejo, México, Oct/31-Nov/3, 2007. CD proceedings paper Nov-13, 1-12 p.

- Hallin M. W., Ball A., Esplín R., and Hsieh K. (2004). *Modal analysis and modeling of highway bridges*, 13th World Conference on Earthquake Engineering, Vancouver, B.C., Canada, August 1-6, paper # 2996.
- Haskell N. A. (1953). *The dispersion of surface waves on multilayered media*, Bull. Seismol. Soc. Am. 43, 17-34.
- Huang C. S. (2000). *Modal identification of structures using ARMV model for ambient vibration measurement*, 12th World Conference on Earthquake Engineering, Auckland, New Zealand, paper # 1702.
- Huerta López C. I., Roësset J. M., Stokoe K. H., and Acosta J. G. (1994). *In-situ determination of soil damping from earthquake records*, A. A. Balkema/Rotterdam/Brookfield (ISBN 90 5410 392 2), Editor S. A. Savidis, Proceedings of the Second International Conference in Earthquake Resistant Construction and Design (ERCAD), 1, 8, 227-234 p.
- Huerta López C. I., Roësset J. M., and Stokoe K. H. (1998). *Evaluation of the random decrement method for in-situ soil properties estimation*, A. A. Balkema/Rotterdam/Brookfield (ISBN 90 5809 030 2), Editors: Kojiro Irikura, Kazuyoshi Kudo, Hiroshi Okada and Tsutomu Sasatani, Proceedings of the Second International Symposium on The effects of Surface Geology on Seismic Motion, Recent progress and new horizon on ESG study, Vol. 2, 749-756p.
- Huerta López C. I., Pulliam J., Nakamura Y., and Yates B. (2001). *Modeling amplification effects of marine sedimentary layers via horizontal/vertical spectral ratios*, Society of Exploration Geophysicist (SEG) (ISSN 1052-3812), Proceedings of the 71st SEG meeting, Vol. 1, 825-828 p.
- Huerta López C. I., Pulliam J., Stokoe K. H., Roësset J. M., and Valle-Molina C. (2003). *Spectral characteristics of earthquakes recorded on the Gulf of Mexico seafloor and soft sediment characterization*, ASME invited lecture at the Offshore Geotechnics Workshop of the 22nd Offshore Mechanics and Arctic Engineering International Conference, (ISBN 0-7918-3672-X), Proceedings of the 22nd Offshore Mechanics and Arctic Engineering 2003 International Conference in CD proceedings, paper # 37504, 1-9p.
- Huerta López C. I., Stokoe K. H., Jay Pulliam, José M. Roësset, and Valle-Molina C. (2005). "Modeling of seafloor soft marine sediments and spectral characteristics of earthquakes recorded on the Gulf of México", *Journal of Offshore Mechanics and Arctic Engineering*, American Society of Mechanical Engineers ASME, (ISSN 0892-7219) 127, 1, 59-67 p.
- Irie Y., and Nakamura K. (2000). *Dynamic characteristics of a r/c building of five stories based on microtremor measurements and earthquake observations*, 12th World Conference on Earthquake Engineering, Auckland, New Zealand, paper # 0500.
- Kanasewich, E. R. (1981). *Time series analysis in geophysics, Third Edition*, University of Alberta Press, Edmonton, Alberta, 480 p.
- Kausel E. and Roësset J. M. (1981). "Stiffness matrices for layered soils", Bull. Seism. Soc. Am. 71. (6): 1743-1761p.
- Midorikawa S. (1990). *Ambient vibration tests of buildings in Santiago and Viña del Mar. Report of the Chilean-Japan Joint Study Project on Seismic Design of Structures*, Sponsor, JICA, Departamento de Ingeniería Estructural, Escuela de Ingeniería, Pontificia Universidad Católica de Chile, Santiago, Chile.

- Minch J. A., Ashby J. R., Demere T. A., and Kuper H. T. (1984). *Correlation and depositional Environments of the Middle Miocene Rosarito Beach Formation of Northwestern Baja California, Mexico*; Minch J.A., Ashby J.R., (eds.), (1984), *Miocene and Cretaceous Depositional Environments, Northwestern Baja California, Mexico*, Pacific Section A.A.P.G., San Diego, California, 54, 33-46.
- Muriá-Vila D., Fuentes O. L., and Gonzáles A. R. (2000). *Uncertainties in the estimation of natural frequencies of buildings in México City*, 12th World Conference on Earthquake Engineering, Auckland, New Zealand, paper # 2092.
- Nakamura Y. (1989). *A method for dynamic characteristics estimation of subsurface using microtremor on the ground surface*, Quarterly Report of Railway Technical Research Institute, 30. (1): 25-33 p.
- Oppenheim, A. V., and R. W. Schafer (1975). *Digital signal processing*. Prentice-Hall, Englewood Cliffs, New Jersey, 556 p.
- Ren W. X., Zatar W., and Harik I. E. (2004). “Ambient vibration-based seismic evaluation of continuous girder bridge”, *Engineering Structures* vol. 26, 631-640 p.
- Rojas R. R., Jara G. J. M., and Hernández B. H. (2006). *Estudio analítico y experimental de un puente peatonal en la ciudad de Morelia*. *Revista Ciencia Nicolaita*, Universidad Autónoma de Morelia, México, 143-140 p.
- Roësset J. M., Huerta López C. I., and Stokoe K. H. (1995). *Effect of magnitude and type of damping in soil amplification*. *University of Missouri-Rolla* (ISBN 1887009019), Editor Shamsher Prakash, Proceedings of the Third International Conference on Recent Advances in Geotechnical Earthquake Engineering and Soil Dynamics. 725-732 p. 04/1995.
- SAP2000 V10. (2000). Computers and structures, Inc.
- SESAME. (2004). Guidelines for the implementation of the H/V spectral ratio technique on ambient vibration: measurements processing and interpretation. <http://sesame-fp5.obs.ujf-grenoble.fr/Delivrables/Del-D23-HVUserGuidelines.pdf>, accessed on Feb/09.
- SESAME European project, (2004). Overall comparisons for test sites. Deliverable D17.10.
- Thomson W.T. (1950). Transmission of elastic waves through a stratified solid medium, *J. Appl. Phys.* 11, 87-180.

APPENDIX A

The power spectrum estimation is calculated using Discrete Fourier Transform (DFT) of each realization (sample) here denoted by $x^{(k)}[n]$, where $n = 0, 1, 2, 3, \dots, N-1$. Each realization is $T = N t_s$ seconds in duration, N denotes the total sample size, and t_s the sampling interval. l^{th} the simple value of the Continuous Fourier Transform (CFT) $X_T(l\Delta f)$ is related to the DFT by

$$X_T(l\Delta f) = \frac{X[l]}{\Delta f}, \dots\dots\dots l = 0, 1, 2, 3, \dots, N-1, \quad (\text{A.1})$$

Where $\Delta f = \frac{1}{T}$. The expression for the k^{th} sampled spectrum, then can be rewritten as

$$S^{(k)}(l\Delta f) = \frac{1}{T} |X_T^{(k)}(l\Delta f)|^2, \quad (\text{A.2})$$

$$S^{(k)}(l\Delta f) = \frac{1}{T} \frac{|X^{(k)}[l]|^2}{(\Delta f)^2}, \quad (\text{A.3})$$

$$S^{(k)}(l\Delta f) = \frac{1}{\Delta f} |X_T^{(k)}[l]|^2. \quad (\text{A.4})$$

$S^{(k)}(l\Delta f)$ is then the PSD representation of the sample. We now introduce the discrete power spectrum $S^{(k)}[l]$,

$$S^{(k)}[l] = S^{(k)}(l\Delta f)\Delta f, \quad (\text{A.5})$$

Combining equations A.4 and A.5, we arrive at the expression for the discrete case of the simple power spectrum,

$$S^{(k)}[l] = |X^{(k)}[l]|^2, \quad l = 0, 1, 2, 3, \dots, N-1, \quad (\text{A.6})$$

where $X^{(k)}[l]$ is the DFT of the k^{th} realization consisting of N samples, for example

$$X^{(k)}[l] = \frac{1}{N} \sum_{n=0}^{N-1} x^{(k)}[n] e^{-i2\pi nl/N}. \quad (\text{A.7})$$

The estimate of the discrete power spectrum $S^{(k)}[l]$ is given by the average of the set of all discrete power spectra. This is,

$$\hat{S}^{(k)}[l] = \frac{1}{M} \sum_{k=1}^M |X^{(k)}[l]|^2, \quad l = 0, 1, 2, 3, \dots, N-1, \quad (\text{A.8})$$

$\hat{S}[l]$ denotes the power associated with those frequencies of bandwidth Δf , centered on $f = l\Delta f$.

AUTHORS BIOSKETCH



S. Hoon

*D*octoral student at Oceanological Research Institute (IIO) of the Autonomous University of Baja California, Mexico. His research interests include the study of dynamic behavior of soils, civil structures vulnerability and natural risk for earthquakes.



C. Huerta-López

*A*ssociate professor and researcher in the Civil Engineering and Surveying Department of the University of Puerto Rico at Mayagüez (UPRM). Experience in industry, teaching and research dates back to the 1980's. His areas of expertise include Earth sciences, Seismology, Geophysics and Engineering seismology. His recent scientific productivity includes 38 publications in referred journals and proceedings with 76 cites out of 21 of these publications, three books, and seven book chapters, and several presentations in conference meetings. He had advised 34 students as supervisor as well as committee member, and from 2007 to current date, he was granted with five research projects by National Council for Science and Technology/México (CONACyT) and private industry also in Puerto Rico. He is member of the Seismological Society of America (SSA), and has the distinction as National Scientific Researcher I since 2006-present, granted by the Mexican government through CONACyT, by the "Sistema Nacional de Investigadores" (SNI).



A. García-Gastélum

*P*rofessor and researcher at the Faculty of Marine Sciences of the Autonomous University of Baja California, Mexico. His main interest is the training of human resources in the assessment of vulnerability and natural risks and environmental indicators. His main research and work are in natural risks assessments like drought, earthquakes, tsunamis and coastal and marine floods, geodiversity studies, at the regional and local levels. Consulting work with municipal, state and federal governments in studies like atlas of municipal natural risks, anti-drought measures program at river basin council level, and management programs. His teaching work is focused on Environmental Indicators, Natural Risks, Remote Sensing and Geographic Information Systems, at the bachelor's, diploma, master's and doctorate levels.